232–242 *Nucleic Acids Research, 2006, Vol. 34, No. 1*
doi:10.1093/nar/gkj423

MSH2 is essential for the preservation of genome integrity and prevents homeologous recombination in the moss *Physcomitrella patens*

Bénédicte Trouiller, Didier G. Schaefer[1], Florence Charlot and Fabien Nogué*

Station de Génétique et d'Amélioration des Plantes, INRA, Route de St Cyr, 78026 Versailles, France
and [1]Département de biologie moléculaire végétale, Université de Lausanne, CH-1015 Lausanne, Switzerland

Received November 18, 2005; Accepted December 14, 2005

ABSTRACT

MSH2 is a central component of the mismatch repair pathway that targets mismatches arising during DNA replication, homologous recombination (HR) and in response to genotoxic stresses. Here, we describe the function of MSH2 in the moss *Physcomitrella patens*, as deciphered by the analysis of loss of function mutants. *Ppmsh2* mutants display pleiotropic growth and developmental defects, which reflect genomic instability. Based on loss of function of the *APT* gene, we estimated this mutator phenotype to be at least 130 times higher in the mutants than in wild type. We also found that MSH2 is involved in some but not all the moss responses to genotoxic stresses we tested. Indeed, the *Ppmsh2* mutants were more tolerant to cisplatin and show higher sensitivity to UV-B radiations. *PpMSH2* gene involvement in HR was studied by assessing gene targeting (GT) efficiency with homologous and homeologous sequences. GT efficiency with homologous sequences was slightly decreased in the *Ppmsh2* mutant compared with wild type. Strikingly GT efficiency with homeologous sequences decreased proportionally to sequence divergence in the wild type whereas it remained unaffected in the mutants. Those results demonstrate the role of PpMSH2 in the maintenance of genome integrity and in homologous and homeologous recombination.

INTRODUCTION

The mismatch repair (MMR) system is evolutionarily highly conserved and plays an essential role in maintaining genome stability (1). In all organisms, MMR is best known for its role in the post-replication repair of DNA polymerization errors. It keeps the rate of mutations due to nucleotide misincorporation and polymerase slippage at an acceptable low level (2). MMR proteins also recognize mismatches in heteroduplex recombination intermediates. In somatic cells, they display an antirecombination activity that inhibits recombination between homeologous sequences present in a single genome (such as allelic genes in diploid cells and members of multigene families) and thus preserves genome integrity (2). This activity also prevents genetic recombination between different but related species and thus contributes to the definition of species. Additionally, MMR plays a role in some types of nucleotide excision repair, which are responsible for repair of physical and chemical damage to DNA. It also participates in a cell-cycle checkpoint control system by recognizing certain types of DNA damage and promoting cell-cycle arrest or triggering apoptosis pathways (3,4).

The methyl-directed MMR system of *Escherichia coli* is composed of MutS and MutL proteins [Mut for mutator phenotype, because they were isolated from mutant strains with high frequencies of spontaneous mutations] (1,3). The MutS proteins are conserved from bacteria to mammals. In eukaryotes MutS homologs (MSH) are encoded by small multigene families, whose members can associate into heterodimers that have discrete roles in MMR-related processes (2). For example, MSH2/MSH6 heterodimers recognize and stimulate the repair of single base-pair mismatches while MSH2/MSH3 heterodimers recognize small insertion/deletion loops (2). The MSH2 protein is a central component of the eukaryotic MMR system and is present in all heterodimers. It is crucial for the repair of all mismatched lesions, whereas other MSH proteins modulate the function of MSH2 depending on the different lesion types or developmental stages.

The *msh2* mutants in yeast and mammals show (i) microsatellite instability, (ii) a mutator phenotype characterized by a

*To whom correspondence should be addressed. Tel: +33 1 30833009; Fax: +33 1 30833319; Email: nogue@versailles.inra.fr
Present address:
Didier Schaefer, Station de Génétique et d'Amélioration des Plantes, INRA, Route de St Cyr, 78026 Versailles, France

high spontaneous mutation rate, (iii) an increased recombination frequency between diverged DNA sequences (homeologous) and (iv) tolerance to certain types of chemical and physical treatments that damage DNA (5–8). In *Caenorhabditis elegans*, loss of MSH2 is associated with microsatellite instability, a mutator phenotype and reduced fertility (9).

However, in plants, the effect of MSH2 mutations is still poorly understood. In *Arabidopsis thaliana*, Hoffman *et al*. (10) have shown rapid accumulation of mutations and microsatellite instability during seed-to-seed propagation of *Atmsh2* defective lines. However, the molecular tools are not available to evaluate the role of MSH2 in the mechanism of homologous recombination (HR) in *A.thaliana* and other higher plants. This type of study in plants is currently only possible in the moss *Physcomitrella patens*.

The moss *P.patens* is unique in the plant kingdom in that it allows high efficiency of gene targeting (GT) via HR (11). Thus, it is possible to use gene knock-out and allele replacement methods in this organism. This allows to examine for the first time the importance of MMR in a multicellular organism in which targeted integration by HR is a major transformation pathway [suggesting that the repair of double strand breaks (DSBs) occurs predominantly by HR]. Recently, we have isolated the *PpMSH2* gene (12). We now have generated *Ppmsh2* disruptants to examine the role of MSH2 in the DNA metabolism of *P.patens*. Here, we show that PpMSH2 is involved in the control of genome integrity and that it is a barrier to recombination between divergent DNA sequences. Furthermore, in the absence of PpMSH2, moss development is dramatically affected most likely as a consequence of a strong mutator phenotype that is directly revealed by the dominance of the haplophase during its development.

MATERIALS AND METHODS

Plant material and culture conditions

The Gransden wild-type strain of *P.patens* (13) was used in this study. Protonemal tissue was propagated on $PpNO_3$ medium (14), supplemented with 2.7 mM NH_4-tartrate (standard medium). Cultures were grown in 9 cm Petri dishes on medium solidified with 0.7% Agar (Biomar) and overlaid with a cellophane disk (Cannings, Bristol). Cultures were illuminated with a light regime of 16 h light/8 h darkness and a quantum irradiance of 80 $\mu E\ m^{-2}\ s^{-1}$ (standard conditions). Sporogenesis was performed in Magenta box in which the tested strains were grown aside the self sterile but cross fertile strain nicB5ylo6 (13) on minimal $PpNO_3$ medium. Crosses were grown in standard conditions for 6–8 weeks (i.e. until about 50 gametophores reached full development), then irrigated with sterile water and transferred for 2 weeks in growth chambers set at 15°C with 10 h of light per day and a quantum irradiance of 15 $\mu E\ m^{-2}\ s^{-1}$. The development of archegonia, antheridia and spore capsules was followed visually during the next month. Antheridia and archegonia were manually dissected for further microscopic observation.

Molecular cloning

We used standard methods for all molecular cloning (15). Using genomic *P.patens* DNA as starting template, we amplified a 2340 bp PCR fragment covering an internal fragment of the *MSH2* genomic region (Gene Bank: DQ117988) and inserted it into the TA-cloning vector pCR®II (Invitrogen, Groningen, The Netherlands) to produce PpMSH2 (oligonucleotide sequences can be provided on request). To obtain PpMSH2-KO, a 465 bp 5′ targeting fragment (coordinate 2557–3022 in DQ117988) and a 598 bp 3′ targeting fragment (coordinate 4614–5212 in DQ117988) were recovered by restriction from PpMSH2 and inserted upstream (5′) and downstream (3′) of the loxP sites flanking the resistance cassette of pBSK35S-NPTII-lox (supplied by Dr Laloue, INRA Versailles). Vector pBSK35S-NPTII-lox carries a neomycin phosphotransferase resistance gene driven by the 35S CaMV promoter and flanked by two LoxP sites in direct orientation. The antibiotic resistance cassette is in the same orientation with regard to the transcription of *PpMSH2*.

To obtain PpAPT-KO, a 3995 bp Xba1 and EcoRI fragment covering the *APT* genomic sequence (Gene Bank: DQ117987), was inserted in pBlueScript KS (Stratagene), forming PpAPT1. The ATG codon is 1217 bp 3′ of the XbaI site and the stop codon is 881 bp 5′ of the EcoRI site in this PpAPT fragment. An internal 1102 bp BamHI fragment was deleted by digestion of the PpAPT1 vector, to produce PpAPTΔ. We generated homeologous variants of this targeting cassette by mutating the PpAPTΔ sequence by mutagenic PCR using the Cadwell and Joyce (16) protocol. Successive APT variants were generated until we reached 3% divergence within the *PpAPT* original fragment. A BamHI fragment containing the hygromycin phosphotransferase gene (*Hpt*II) driven by the 35S CaMV promoter was recovered from plasmid pGL2 (17) and ligated into the BamHI site of PpAPTΔ and of the variants to produce the homologous and homeologous PpAPT-KO vectors (Figure 4).

Protoplasts isolation and regeneration

Protoplasts were isolated from 6-day-old protonema by incubation for 40 min in 1% Driselase (Fluka 44585) dissolved in 0.47 M mannitol. The suspension was filtered successively through 80 and 40 μm stainless steel sieves. Protoplasts were sedimented by low-speed centrifugation (600 *g* for 5 min at 20°C) and washed twice with 0.47 M mannitol. Protoplasts were then resuspended at 1.2×10^6 protoplasts/ml in MMM solution (0.47 M mannitol, 15 mM $MgCl_2$ and 0.1% MES, pH 5.6) for transformation. For growth assay and phenotypic analyses, protoplasts were resuspended at a density of ca. $1–3 \times 10^4$ protoplasts/ml in mannitol 0.47 M containing 0.5% agar. Two ml of suspension were spread on cellophane disks covering standard medium supplemented with 0.5% glucose and 0.36 M mannitol (PPM). Regeneration was conducted in standard growth conditions. After 1 week of regeneration, protoplasts were transferred to standard medium without mannitol.

Transformation of protoplasts

Moss protoplasts (1.2×10^6) were transformed as described previously (18) with PpMSH2-KO digested with AgeI and AatII, which generate DSBs within the genomic *MSH2* sequence. Primary transformants were selected in the presence of 50 mg/l paramomycin (Duchefa P0141, Haarlem, The Netherlands). Small pieces of the protonema tissue (~2 mm

in diameter) of primary *P.patens* transformants were then transferred onto standard medium without selection and cultured for 15 days. A second round of selection allowed the isolation of stable transformants, by transferring small pieces of protonema tissue from the previous colonies onto standard medium containing 50 mg/l G418 (Duchefa G0175, Haarlem, The Netherlands) (paramomycin and G418 belong to the kanamycin family of antibiotics).

Molecular analysis of Msh2 knockouts

Moss DNA was extracted from 200 mg of fresh protonema tissue ground in 220 µl of extraction buffer (220 mM Tris–HCl, pH 7.5, 250 mM NaCl, 25 mM EDTA and 0.5% SDS) with an electric pestle in the presence of sand. After centrifugation, DNA was precipitated with isopropanol at room temperature. The pellet was dried and resuspended with 100 µl sterile water. Stable disruptants of the *PpMSH2* gene were screened by PCR for the incorporation of the resistance cassette into the *MSH2* locus. We used primers specific for the resistance cassette (Uc: TATTTTTGGAGTAGACAAGCGTGTCGT and Lc: CCGCTTCCTCGTGCTTTACGGTAT) and primers specific for the *PpMSH2* sequence outside the transformation construct (PpMSH2#4: CAATGTCACTGAGAGCAAAACG and PpMSH2#5: CACACTGATCTCTGCTCGGTCG).

Moss RNA was isolated using the RNAeasy kit (Qiagen) starting with 100 mg of fresh protonema. We obtained doubled-stranded cDNAs corresponding to mRNAs expressed in 6-day-old protonema cultures using the SMART-PCR cDNA Synthesis Kit (Clontech). The primers PpMSH2#4 and PpMSH2#2 (CACCAACACGCGCAAAGATG) were used for PCR on these cDNAs.

Generation of clean deletion by transient Cre recombinase expression

Direct repeats of LoxP recombination sites from the Cre/lox system (19) were located on either side of the 35S-nptII resistance cassette in PpMSH2-KO. Transient expression of a constitutive Cre expression cassette (20) in protoplasts allowed excision of the resistance gene from the *PpMSH2* recombinant locus (D.G. Schaefer, A. Finka and J.P. Zrÿd, manuscript in preparation). Protoplasts were regenerated at a low density on non-selective medium for 2 weeks and fragments of single protoplast-derived colonies were then replicated on selective (i.e. G418 50 mg/l) and non-selective medium. Loss of antibiotic resistance was determined after an additional week of growth. Replicates growing on non-selective medium were used for subsequent amplification and molecular analyses. Clone *Ppmsh2*Δ was selected this way and used for further analyses. We analyzed by PCR the recombinant locus with the primers PpMSH2#4 and PpMSH2#2.

Cytology

Binocular observations were made with a Nikon SMZ1000, and microscopic observations with a Leitz (type 090-122.012) inverted microscope.

Evaluation of spontaneous mutation frequency

Mutations in the *APT* gene confer resistance to 2-FA (2-Fluoroadenine, from Dr Laloue, INRA Versailles, France), a toxic compound for cells. The number of 2-FA resistant colonies reflects the frequency of spontaneous mutations. Protoplasts of wild-type and *Ppmsh2* mutants were regenerated for 6 days regeneration on PPM ($\sim 10^5$/Petri dish) and then transferred on standard solid medium supplemented with 10 µM 2-FA. After 2 weeks, the number of resistant colonies was counted. We repeated this experiment three times. The *APT* genomic sequence from 2-FA resistant clones was subsequently PCR amplified and sequenced to identify the mutation responsible for the resistance (oligonucleotide sequences can be provided on request).

Sensitivity to cisplatin/MNU and γ/UV-B radiations

Cisplatin (*cis*-diamminedichloroplatinum(II)) (Calbiochem, Darnstadt, Germany), MNU (N-methyl-N-nitrosourea) and O^6-bzGua (O^6-benzylguanine) (Sigma-Aldrich, Steinheim, Germany) were dissolved in dimethyl sulfoxide at 100 mM each for storage at −20°C and at 25 mM for O^6-bzGua immediately before use.

Wild-type and *Ppmsh2* mutant protoplasts in liquid PPM were treated for 20 h with 0–5 mM cisplatin or MNU (2×10^5 protoplasts at each concentration). From 1 h before exposure to MNU and throughout the whole procedure, 25 µM O^6-bzGua was present in the medium to inhibit the removal of methyl groups from the O^6 position of guanine by endogenous methyl-transferase activity. After 20 h in the dark, protoplasts were washed and spread on solid medium at low concentrations.

Protoplasts in liquid mannitol medium were exposed to ionizing radiation (1 Gy/s) using a ^{137}Cs irradiator (IBL-637 CIS-Bio-International, Institut Curie, Orsay). After 20 h in the dark, the protoplasts were spread on solid medium at low concentrations.

Protoplasts spread on solid medium (5×10^4 protoplasts at each concentration in four Petri dishes) were exposed to UV-B light (60 J/m^2/s) from a 312 nm TFX lamp. We calculated the flux with a UV-Elektronik GmbH dosimeter. The protoplasts were then left in the dark for 20 h.

After 6 days regeneration, protoplasts were transferred onto standard solid medium. After 1 week, the number of survivors was counted. We repeated these experiments two to three times. Statistical analyses have been made with the χ^2 test.

APT targeting frequency with homologous and homeologous DNA

Targeting *APT* fragments were produced by digestion of PpAPT-KO vector with NotI and EcoRI enzymes. We selected stable transformants after transformation of wild-type and *Ppmsh2* mutant protoplasts with homologous and homeologous *APT* disruption fragments. Small pieces of protonema tissue (~2 mm in diameter) from stable transformants were then transferred onto standard medium containing 10 µM of 2-Fluoroadenine to detect *APT* gene targeting events. Experiments were repeated three times.

RESULTS

Targeted disruption of the MSH2 gene in *P.patens*

Moss protoplasts were transformed with vector PpMSH2-KO and four independent clones were selected for further

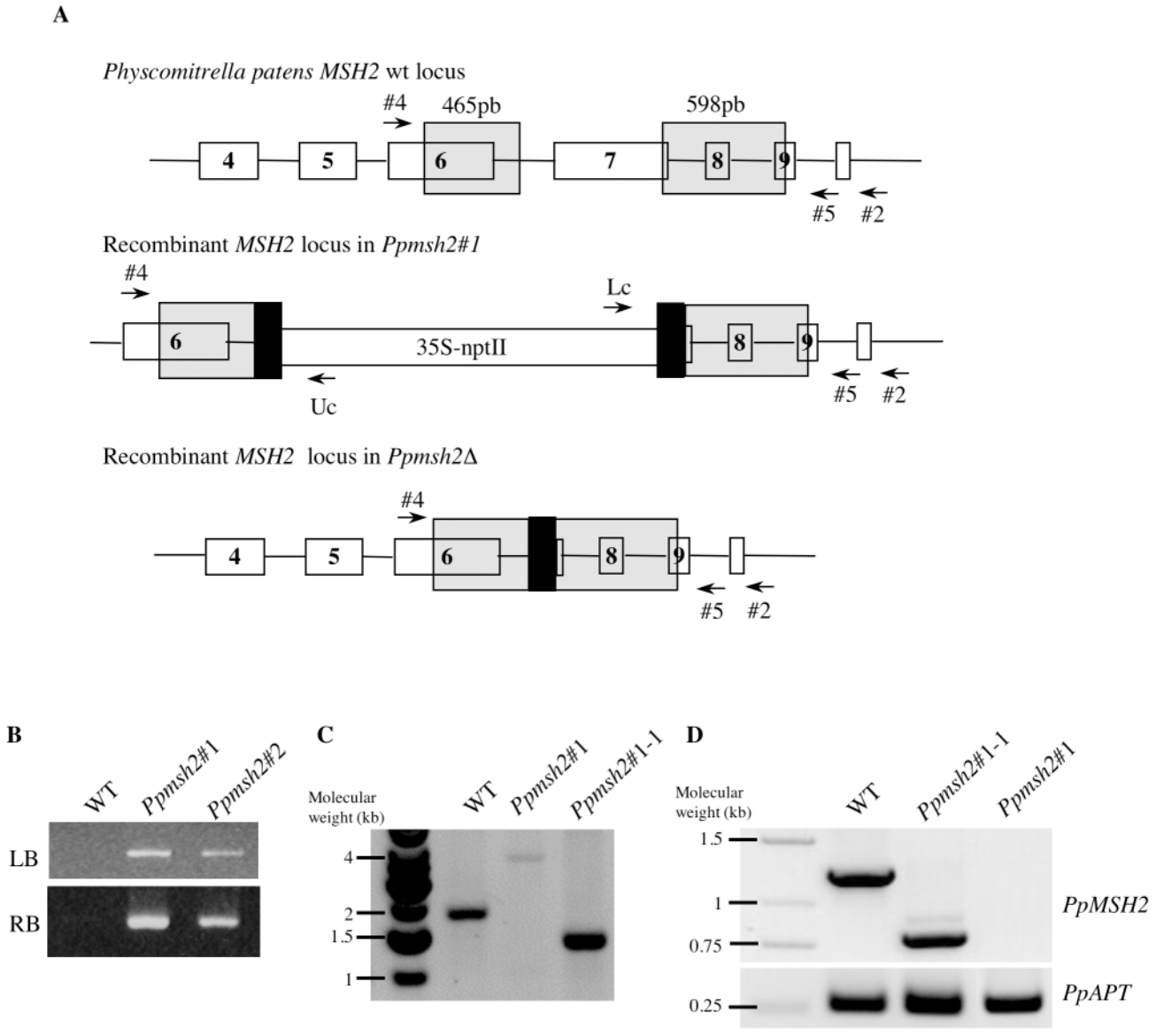

Figure 1. Molecular analysis of *Ppmsh2* mutants. (**A**) Schematic representation of *PpMSH2* genomic locus, schematic representation of *PpMSH2* disrupted locus with a double crossover insertion and schematic representation of *PpMSH2* disrupted locus without resistance gene. Black open boxes represent exons, black lines represent introns, gray open boxes are homology regions used to disrupt the gene, black boxes are Lox sites for Cre recombination and arrows show the primers used for PCR. *Ppmsh2Ø* is mutant without the resistance gene, resulting from *Ppmsh2#1* after Cre recombinase expression. (**B**) PCR of the recombinant borders with a primer external to the targeting sequences and one on the resistance gene [primers: PpMSH2#4/Uc for left border (LB) and Lc/PpMSH2#5 for right border (RB)]. (**C**) PCR with primers flanking recombination sites (primers: PpMSH2#4/2), (**D**) RT–PCR for *PpMSH2* transcripts (primers: PpMSH2#4/2), *PpAPT* was used as control.

investigation (*Ppmsh2#1* to *Ppmsh2#4*). In each clone, disruption of the chromosomal *PpMSH2* locus was controlled by PCR and absence of the *PpMSH2* transcript was established by RT–PCR (see *Ppmsh2#1* for example Figure 1B–D). In order to obtain a simple deletion mutant, the resistance cassette inserted at the *PpMSH2* locus of the *Ppmsh2#1* clone was eliminated by the CRE recombinase to produce clone *Ppmsh2*Δ (see Materials and Methods and Figure 1A). In this clone, we confirmed deletion of exon 7 of the *PpMSH2* gene by PCR and checked modification of the transcript by RT–PCR (Figure 1C and D). The four independent *PpMSH2* knockouts (*Ppmsh2#1* to *Ppmsh2#4*) and the deletion mutant (*Ppmsh2*Δ) behaved identically under all circumstances tested except in aged cultures. Therefore, *Ppmsh2*Δ mutant was used for further characterization except for late developmental phenotypes (see below). To avoid the genetic drift resulting to the expected mutator phenotype associated with *msh2* mutations, all the experiments were performed using the primary stock of protonema suspension from *Ppmsh2*Δ stored at 4°C as starting material.

Ppmsh2 mutants display pleiotropic developmental defects

The haploid gametophytic development of *P.patens* from regenerating protoplasts starts with a filamentous branched structure called the protonema that grows by apical cell divisions and lateral division of subapical cells. There are two cell

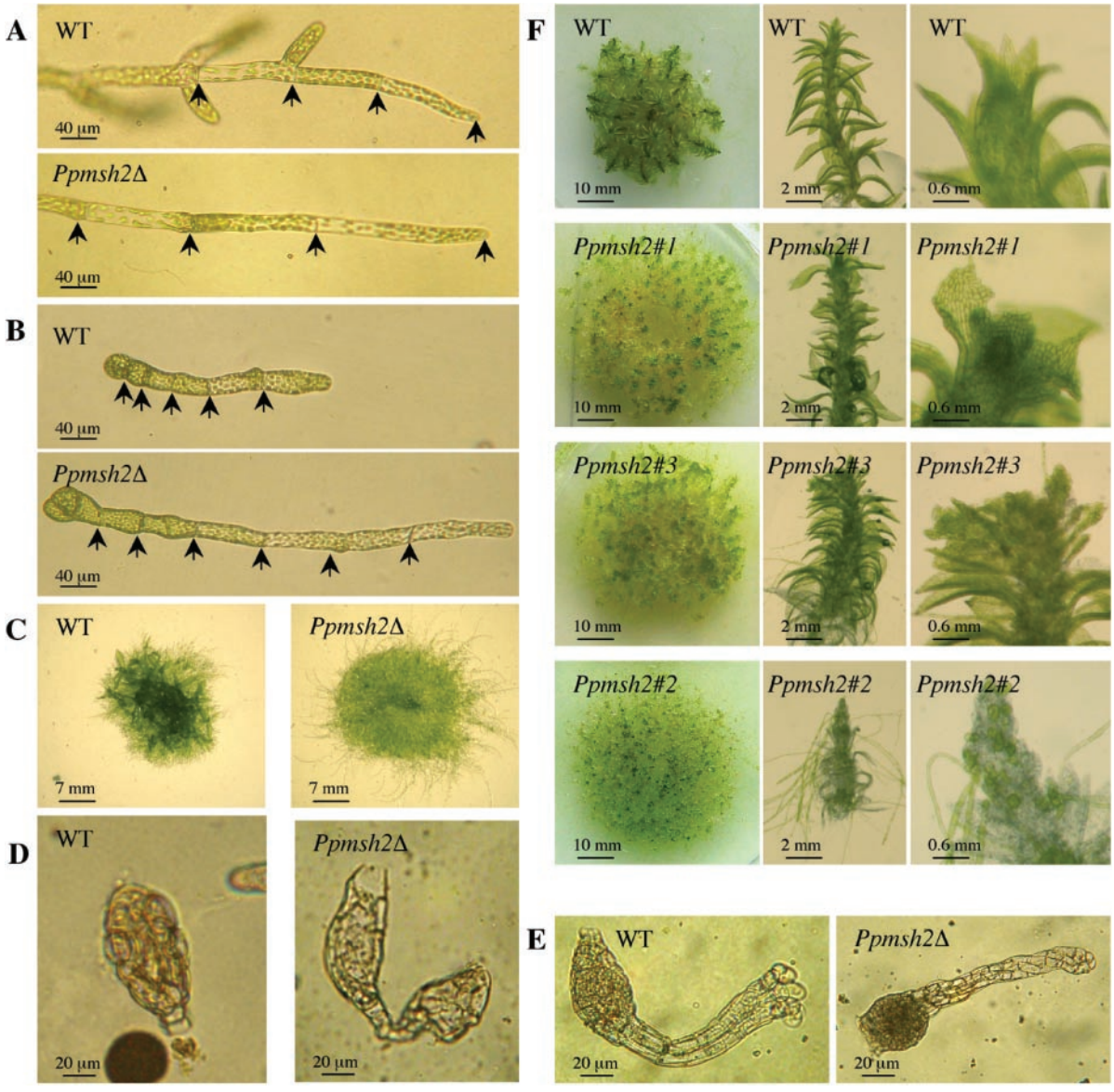

Figure 2. Comparison of wild type and *Ppmsh2* mutants apparent phenotypes: (**A**) Comparison of the length of the last three cells of protonema filaments; arrows show the cell walls. (**B**) Number of cell divisions after 8 days protoplast regeneration; arrows show the cell walls. (**C**) Wild-type and *Ppmsh2*Δ mutant colonies after 3 weeks development. (**D**) Male antheridia of wild-type and of *Ppmsh2*Δ mutant, (**E**) female archegonia of wild-type and of *Ppmsh2*Δ mutant. (**F**) Wild-type, *Ppmsh2#1*, *Ppmsh2#3* and *Ppmsh2*#2 mutant colonies after 12 weeks development, a representative leafy shoot from those colonies and enlargement of the top of the same gametophore.

types in protonema filaments: chloronema and caulonema. Regenerating protoplasts first develop into photosynthetically active chloronemal filaments, formed by cells filled with chloroplasts and separated by walls perpendicular to the axis of the filaments. After ~5 days, chloronemal apical cells occasionally differentiate into caulonemal cells characterized by oblique cell walls and smaller and fewer chloroplasts. After 8–10 days, primitive meristems called buds differentiate from caulonemal side branch initials and further differentiate into leafy shoots, also known as gametophores. Each leafy shoot resembles a small plant with an unbranched stem, filamentous basal and aerial rhizoids and leaves displaying clear phyllotaxis along the stem axis (21). We found that the *msh2* mutants had several pronounced phenotypes affecting the development of both protonema and leafy shoots.

Gametophytic developmental failures. Preliminary observations of *msh2* mutant colonies regenerated from protoplasts indicated that these colonies were larger than those obtained from wild-type protoplasts (data not shown). To further quantify this observation, we compared the size of protonema filaments by measuring the length of the three apical cells from 14-day-old regenerated colonies. We found a significant difference in the mean length between the wild-type and the *Ppmsh2*Δ mutant (4.2 ± 1 versus 7.2 ± 2, arbitrary units, *t*-test $P < 0.0001$, $n = 40$) (Figure 2A). These data suggest that the *Ppmsh2*Δ mutant cells elongate 1.5 times faster than the wild-type cells. We next evaluated the cell division rate in the two backgrounds by counting the number of cell divisions after 8 days from regenerated protoplasts. We found a significant difference for mean cell division numbers between the

wild-type and for the *Ppmsh2*Δ mutant (5 ± 0.5 versus 6 ± 0.8, *t*-test $P < 0.0001$) (Figure 2B), showing that the number of cell divisions was slightly increased in the mutant.

Differentiation of chloronema cells into caulonema cells looks normal in the mutant compared with wild type. After 10 days of growth, differentiation of buds and further development of leafy shoots could clearly be observed in WT colonies whereas, at the same time-point, the *Ppmsh2*Δ mutant colonies had neither developed buds nor leafy shoots and the protonema was more widespread (data not shown). After 3 weeks, wild-type colonies had numerous well-developed leafy shoots, whereas *Ppmsh2*Δ filaments had just developed a few leafy shoots that were thinner, shorter and occasionally distorted (Figure 2C). We therefore concluded that loss of function of MSH2 seriously impairs the normal development of *P.patens* at different levels: protonema cell growth is accelerated, protonema cell cycle may be shorter, differentiation of buds is delayed and further development of leafy shoots is architecturally affected.

Reproductive developmental failures. The late developmental stages of *P.patens* life cycle are the differentiation of reproductive organs, fertilization to produce the diploid sporophyte and meiosis of spore mother cells to produce haploid spores. Therefore, we examined whether the developmental abnormalities seen at the protonema and leafy shoot stages could also be observed in antheridia (male) and archegonia (female), the reproductive organs of *P.patens* that differentiate at the apex of leafy shoots. After 10 weeks, the reproductive organs of wild type were fully developed on leafy shoot (Figure 2D and E) and the sporophyte further developed normally to produce viable spores (data not shown). In all five *Ppmsh2* mutants, abnormal reproductive organs were formed on the few leafy shoots (Figure 2C), with aberrant number and shape of cells (Figure 2D and E). Consequently we never obtained differentiated capsules from the mutants and concluded that loss of function of MSH2 led to complete sterility in *P.patens*. To determine whether sterility was due to a problem in male and/or female gametes, reciprocal out-crosses were performed between *Ppmsh2* mutants and strain NicB5ylo6. We did not obtain any capsules from these crosses and thus concluded that *Ppmsh2* mutants were male and female sterile as a consequence of abortive development of reproductive organs.

Late developmental defects. In order to check the phenotype of late growing colonies, we inoculated similar size filaments (5–10 cells) from 3-week-old single protoplasts derived colonies on standard medium. After 6 weeks, the mutant colonies started to become chlorotic and a significant fraction of the cells were dead (data not shown). After 12 weeks, wild-type colonies were healthy (Figure 2F, WT) whereas those from independent *Ppmsh2* knockouts presented various developmental aberrations from leaf shape abnormalities (Figure 2F, *Ppmsh2#1*) or supernumerary leaves and 'callus'-like structure (Figure 2F, *Ppmsh2#3*) to completely disorganized necrotic shoots with numerous aerial rhizoids (Figure 2F, *Ppmsh2#2*). Additionally, the frequency of dead cells in these colonies was directly proportional to the intensity of the phenotype. In the most dramatic case (*Ppmsh2#2)* the leafy shoots were completely dead since isolated gametophores plated on fresh standard medium were not able to regenerate viable protonema, which was feasible with WT leafy shoots isolated from the same culture (data not shown). We also observed that the intensity of the phenotypes increased proportionally to the number of subcultures the original clone has undergone (data not shown), suggesting that random mutations accumulated within *Ppmsh2* mutant clones in successive subcultures. Those late phenotypes could clearly be associated with major developmental processes, such as the establishment of shoot architecture, early senescence and eventually active cell death. The diversity of the phenotypes observed in *Ppmsh2* mutants supports a strong mutator phenotype that is immediately detected in the moss haploid gametophyte. For this reason all the following experiments have been carried out using 3–4 individual replicates of the primary isolated knockout clones (stored at 4°C) as starting material.

Ppmsh2 mutants have a mutator phenotype

The strong developmental defects observed in *Ppmsh2* mutants could be related to accumulation of spontaneous mutations. This phenotype has already been observed in *msh2* mutants of other organisms (2). To further quantify this mutator phenotype, we investigated the effect of the loss of the *PpMSH2* gene on mutation frequency of the adenine phosphoribosyl transferase (*PpAPT*) reporter gene. Spontaneous mutations leading to loss of APT activity confers resistance to adenine analogues, such as 2-fluoroadenine (2-FA) and can be selected on standard medium supplemented with 10 μM 2-FA. We tested a total of 10^7 *Ppmsh2*Δ protoplast-derived colonies and 3×10^6 wild-type colonies for resistance to 2-FA.

We observed no resistant colonies in the wild type and a total of 398 2-FA resistant colonies in the *Ppmsh2*Δ mutant. *APT* mutation frequencies were thus lower than 3×10^{-7} in wild type and $4 \times 10^{-5} \pm 1.2 \times 10^{-5}$ in *Ppmsh2*Δ. To confirm that 2-FA was effectively resulting from mutation in the *APT* gene, we partially sequenced the *APT* gene of randomly chosen 2-FA resistant clones. Point mutations in the *APT* sequence were effectively detected in more than 75% of the clones tested (Table 1). Mutations resulting from transitions and transversions were recovered, but we did not identify mutations resulting from insertion or deletion. These modifications were matching with highly conserved domain or amino acid of the APT protein and some of them were identified several

Table 1. Point mutations identified in the *APT* genomic sequence in *Ppmsh2*Δ 2-FA resistant clones

Genomic position[a]	Amino acid[b]	DNA mutation	Consequence[c]
1447	28	GGC→TGC	Intron I splicing
1462	33	GAT→TAT	D→T
1559	65	GGT→GAT	G→D
1687	Intron II	AGG→ATG	Intron II splicing
2121	108	GGT→GAT	G→D
2195	133	GCC→ACC	A→T
2464	150	GCG→GAG	A→E
2485	157	TGC→TAC	C→Y

[a]Position 1 corresponds to the first nucleotide in the genomic *PpAPT* sequence DQ117987.
[b]Position 1 corresponds to the ATG codon in the PpAPT protein.
[c]Universal genetic code for amino acid.

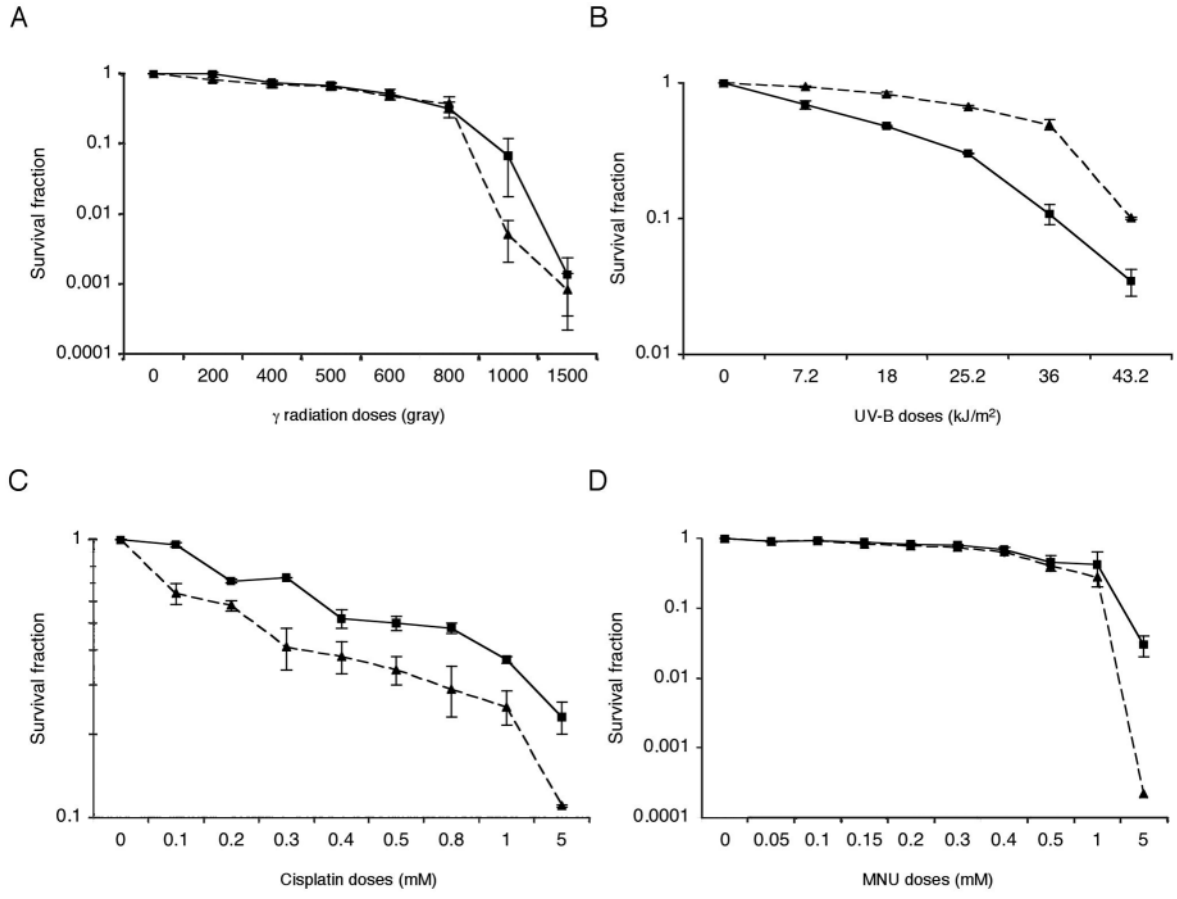

Figure 3. Survival fraction after different genotoxic stresses. (**A**) γ-radiation, (**B**) UV-B, (**C**) Cisplatin, (**D**) MNU. Wild-type survival is represented with triangles and dashed line, and *Ppmsh2*Δ mutant survival is represented with squares and solid line. Error bars indicate SD based on at least two independent experiments in all cases.

times in independent 2-FA resistant clones. These results demonstrate that loss of *MSH2* gene leads to the accumulation of point mutations in the moss genome and that the spontaneous mutation rate is increased at least by two orders of magnitude (130 times) in the *Ppmsh2*Δ mutant compared with the wild type. This last value is probably underestimated since the screen used here has selected only mutations that confer 2-FA resistance. Additionally, the type of mutations identified suggests that they result from defaults of post DNA replication proofreading processes.

Msh2 mutants display altered responses to genotoxic stresses

MMR is known to recognize different types of DNA damages depending on the lesion and on the organism. MMR is responsible for the hypersensitivity to agents, such as radiation or some genotoxic chemicals that create DNA lesions (22). Loss of MMR may prevent cell death normally resulting from exposure to such genotoxic agents, thus conferring tolerance to these stresses. Therefore, we treated *Ppmsh2*Δ mutant protoplasts with UV-B and γ-radiation and chemicals such as cisplatin and MNU to determine whether *P.patens* cells with defective MMR would be affected or not. Survival was calculated as the ratio of protoplasts surviving after 15 days regeneration following treatment to the number of protoplasts undergoing normal regeneration without treatment.

Ppmsh2 mutants are equally sensitive to γ-radiations than wild type. Ionizing radiation can cause many different lesions in DNA, including strand breaks and base or sugar damage (23,24). Oxidized base damages induced by ionizing radiation may therefore be substrate for MMR (22). We compared the effect of γ-radiation on the survival of *Ppmsh2*Δ mutant and wild-type protoplasts. We found that both wild-type cells and *Ppmsh2*-deficient cells were similarly affected by γ-radiation (Figure 3A). For both genotypes, the LD_{50} (Lethal Dose 50%) was reached at 600 Gray. All γ-radiation dose comparisons were not significantly different.

Ppmsh2 mutants are more sensitive to UV-B radiations than wild type. A high UV-B flux can introduce a number of different lesions into the genome, mostly cyclobutane pyrimidine dimers (CPDs) and pyrimidine-6-4-pyrimidinone adducts (6-4PPs) (25). The elimination of these DNA photoproducts is essential for cell survival because both RNA- and DNA-polymerase are unable to read through both of these classes of dimers. Therefore, we tested the effect of increasing UV-B doses on the survival of regenerated wild-type and *Ppmsh2*Δ mutant protoplasts. We found that wild-type protoplasts were

affected by high doses of UV-B, with an LD_{50} of 36 KJ/m^2. In the *Ppmsh2*Δ background, the lethal dose was only 18 KJ/m^2 (Figure 3B). All UV-B dose comparisons were significantly different. These results show that the *Ppmsh2*Δ mutant is more sensitive to UV-B than the wild type.

Ppmsh2 mutants are more tolerant to cisplatin than wild type. Cisplatin is a DNA-damaging drug that forms bifunctional covalent adducts with DNA and is a well-recognized mutagen that affects the survival of mammalian cells (26). We compared survival of wild-type and *Ppmsh2*Δ mutant regenerated protoplasts after exposure to increasing concentrations of cisplatin. The LD_{50} for the wild type was 250 μM cisplatin (Figure 3C), whereas the *Ppmsh2*Δ cells were more resistant than wild-type cells, with an LD_{50} of about 500 μM. All concentration comparisons were significantly different. These experiments show that the *Ppmsh2*Δ moss cells have a cisplatin tolerant phenotype.

Ppmsh2 mutants are more tolerant to MNU than wild type. The cytotoxicity of methylating agents such as MNU (*N*-methyl-*N*-nitrosourea) is primarily caused by their ability to introduce O^6-methylguanine (O_6-meGua) into the DNA (27). Persistent O^6-meGua in the DNA is normally lethal. Therefore, we determined survival of wild-type and *Ppmsh2*Δ mutant cells after exposure to increasing concentration of MNU. Wild-type survival was slightly affected by 1 mM MNU and dramatically affected by 5 mM MNU treatment. These values are comparable with those reported for MNU-induced DNA damage in Barley (28). The survival of *Ppmsh2*Δ mutant cells was slightly better than wild type at 1 mM MNU and significantly higher at 5 mM (Figure 3D). The LD_{50} was reached at 500 μM for both genotypes. These results show that *Ppmsh2*Δ moss cells have a weak resistance to MNU at high doses.

Gene targeting is decreased and homeologous recombination is not repressed in *Ppmsh2* mutants

In *E.coli* (29), *Saccharomyces cerevisiae* (5), *Trypanosoma brucei* (30) and mouse embryogenic stem cells (7), depletion of MutS or *MSH2* leads to an increased frequency of recombination between homeologous DNA sequences. We examined the involvement of PpMSH2 in HR by measuring GT efficiency with homologous or homeologous DNA sequences at the *APT* locus. Wild-type and *Ppmsh2*Δ cells were transformed with *APT* constructs presenting 0, 1, 2 and 3% divergence to the *PpAPT* genomic sequence, respectively (Figure 4). Hygromycin resistant transgenic clones were initially selected and tested for 2-FA resistance. GT frequency was calculated as the ratio of 2-FA resistant clones to the total number of Hygromycin resistant transformants.

We observed a significant decrease (1.8-fold) in GT frequency for mutant cells compared to wild type ($P = 0.001$) when the recombination substrate was fully homologous to its genomic target (Table 2). In wild type, GT frequency decreased as the percentage of divergence increased, whereas GT frequency remained stable for the *Ppmsh2*Δ mutant whatever the divergence level (Table 2). In wild type GT frequency significantly decreased 22-fold with 3% mismatches compared to 0% mismatches (χ^2 test, $P < 0.00001$), whereas in *Ppmsh2*Δ mutant, the GT was as efficient with homeologous fragments as with homologous fragment ($P = 0.40$). Thus, GT efficiency with a homeologous fragments containing 3% divergence was increased 15-fold in *Ppmsh2*Δ mutant compared to the wild type. These data demonstrate that loss of function of *MSH2* allows GT in *P.patens* with up to 3% divergent homeologous sequences, hence that the moss MSH2 protein has an antirecombination activity that prevents recombination between slightly divergent sequences.

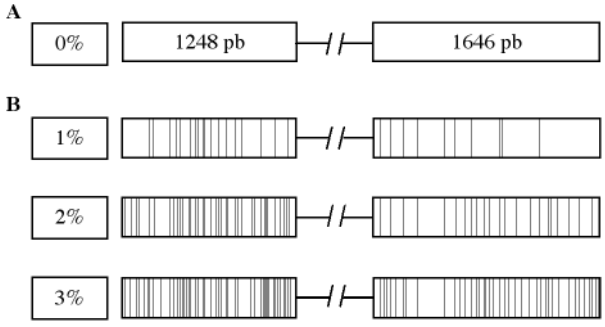

Figure 4. Gene targeting PpAPT fragments used for homologous and homeologous recombination studies. The hygromycin gene resistance cassette is represented between both PpAPT fragments by a horizontal interrupted line. (**A**) PpAPT fragments in the PpAPT-KO cassette in which the sequences are exactly identical to the locus *PpAPT* used as reporter gene. (**B**) Alignments of PpAPT fragments in homeologous recombination cassettes; each vertical line indicates mismatch between mutated *PpAPT* fragments and the original locus.

Table 2. Gene targeting frequency in wild type and *Ppmsh2*Δ mutant

Divergence (%)	Genotypes Wild type	*Ppmsh2*Δ
0	44% (90/204)[a]	24% (68/278)[a]
1	14% (11/81)[a]	31% (14/45)[a]
2	9% (4/46)[a]	20% (4/20)[a]
3	2% (2/124)[a]	30% (29/96)[a]

aPercentages correspond to GT frequency, which is the number of 2-FA resistant clones divided by the number of stables hygromycin resistant clones, indicated in brackets.

DISCUSSION

Ppmsh2 mutants show strong developmental defects, are sterile and have a mutator phenotype

Ppmsh2 mutant colonies develop strong developmental defects, including sterility, after a few weeks. This sterility may be due to the *msh2* associated mutator phenotype increasing the rate of mutations that cause developmental problems in complex structures such as leafy shoots, antheridia and archegonia. Similar phenotypes have been observed in *Arabidopsis thaliana msh2* mutant lines (10). After five generations, plants showed abnormalities in morphology and development, fertility, germination efficiency, seed/silique development and seed set. In human and mice, mutations in *MSH2* result in a greatly increased likelihood of developing certain types of tumors (31). As in other eukaryotes, during growth and development, MSH2 in moss seems to be essential for the maintenance of genome integrity. Accordingly, we scored a 130-fold increase in the spontaneous mutation rate

of the *APT* gene in *Ppmsh2* mutants compared with wild type. This increased mutation rate is comparable with those observed in *E.coli mutS* mutant (20-fold increase) (32), or *S.pombe* (15-fold increase) (33) and *S.cerevisiae* (200-fold increase) (8) and other higher eukaryotes *msh2* mutants (from 30- to several hundred-fold increase (7,10,34,35). This mutation rate can explain the phenotypes observed in the *Ppmsh2* mutants. Assuming that the amount of mutations increases with the number of rounds of DNA replication, abnormalities should increase with the number of generations of vegetative propagation and this is what we observed after multiple successive subcultures of the colonies. Nevertheless, the phenotypes we observed in the mutant background are particularly strong, and two explanations can be proposed to account for this observation. The first one is linked to the fact that the major part of the moss life cycle is haploid. Thus, the deleterious effects of mutations in development are greater in moss than for diploid mice or *A.thaliana*, where the allelic locus would mask the phenotype resulting from randomly occurring mutations, at least in the first generation. Moreover, we cannot discard the hypothesis that, as in budding yeast, efficient GT in *P.patens* reflects the predominance of the HR pathway in the repair of DNA DSB. In this case, alteration of the MMR system, which participates in this DNA repair pathway, would lead to more drastic effects than in other higher eucaryotes, where HR is not the major pathway for DNA DSB repair. This is reminiscent of the strong reduction in spore viability observed in the *msh2* yeast mutant (36) an organism where HR is also predominant.

Is PpMSH2 protein involved in cell-cycle checkpoints and apoptosis-induced by genotoxic stresses?

The sensitivity of cells to agents that create lesions on DNA has been attributed to attempts of MMR to correct the resulting damage (22). Depending on the type of DNA damage, loss of MMR may result in increased mutagenesis, loss of cell-cycle control and resistance to apoptosis (37). The resistance of *msh2*-deficient cells to DNA damage is not so clear because it depends on the organism and on the specificity of the lesions. In *C.elegans*, MSH2 confers sensitivity to ionizing radiation (9). In mouse cells, conflicting results have been reported, although the effects are generally minor. Msh2-nullizygous cells were found to exhibit slight higher levels of survival after exposure to ionizing radiation (38,39). However, it has recently been shown that both mouse embryogenic fibroblasts (MEFs) and mouse colorectal carcinoma cells defective in MSH2 were slightly more sensitive (1.5-fold) to X-ray irradiation than their MSH2-non-defective counterparts (40). In contrast, in moss, as in drosophila and human cells, the loss of MSH2 does not affect the sensitivity to γ-radiation, suggesting that MSH2 is not involved in the detection of lesions due to γ-radiation (41,42).

In *E.coli, T.brucei*, mouse and human cells, MSH2 confers sensitivity to MNU (27,38,43,44). In contrast, in the yeast *S.cerevisiae*, the MMR system did not affect sensitivity to methylating agents (45). In our experiments, *Ppmsh2* mutants showed only a weak resistance to MNU at high concentration. This suggests that only a fraction of the MNU cytotoxicity in moss cells may be dependent on MSH2 function. Other mechanisms must be involved to repair DNA lesion in conjunction or not with MMR. HR can repair DNA lesions, like it has been shown in yeast for O^6-meGua damages (45). Absence of MMR in *S.cerevisiae* did not affect sensitivity to methylating agents, while HR inactivation sensitized cells to this agent. In HR-deficient cells, defects in the *MSH2* gene rescue the original sensitivity (45). These authors conclude that methylation damage processing and repair by HR masks the sensitivity of MMR-proficient *S.cerevisiae* cells toward methylating agents (45). In our experiments, *Ppmsh2* mutants showed a weak resistance to MNU only at high concentration, suggesting that only a fraction of the MNU cytotoxicity in moss cells may be dependent on MSH2 function. Like in yeast, moss MMR could be overwhelmed by other mechanisms such as HR, thus preventing the cytotoxicity due to methylating agents to be detectable in wild type.

Peters *et al*. (37) have shown that in MEF (mouse embryogenic fibroblasts), MSH2 may sense damage due to photoproducts or may contribute to the processing of UV-B-induced DNA damage, thereby initiating apoptosis and influencing the activation of p53 (a tumor suppressor which functions as a transcription factor involved in cell-cycle checkpoints and apoptosis). They showed that *Msh2*-null MEFs were partially resistant to the cytotoxic effects of UV-B, and that this resistance led to a reduction in apoptosis. In contrast, we have shown that the *Ppmsh2* mutant is more sensitive to UV-B radiation than the wild type. Therefore, MSH2 in moss may play a more important role in the recognition of UV-B lesions than that reported in MEF.

Experiments in *E.coli* have shown that loss of MMR activity, due to mutations in *mutS*, was correlated with cisplatin resistance (46,47). There are conflicting results in the response of cisplatin treatment in higher eukaryotes. It was thought that mouse MSH2 conferred sensitivity to cisplatin (48). However, Claij and te Riele (49) have recently shown that *msh2*-deficient mouse cells do not respond specifically to cisplatin lesions compared with wild type (49). In contrast, data from *Trypanosoma cruzei* have demonstrated a role of MSH2 in sensitivity to cisplatin (50), like in prokaryotes and in yeast (46,51). Our results in moss show that *Ppmsh2* mutants are tolerant to cisplatin.

The fact that *Ppmsh2* mutants have opposite responses to lesions due to UV-B (sensitivity) and cisplatin (resistance) suggests that moss may have different pathways for managing lesions involving PpMSH2 proteins. PpMSH2 may signal DNA lesions and induce cell-cycle arrest followed by either DNA repair or apoptosis to prevent accumulation of a large number of mutations. In the absence of PpMSH2, we suggest that, depending on the type of DNA lesions, different responses may be engaged. When the lesion is too severe (exposure to UV-B), the cells are unable to repair them and die. For other lesions, they can be bypassed by a translesion synthesis polymerase (52,53) or be repaired by other mechanisms such as base excision repair, nucleotide excision repair or by HR (45,54,55). In these cases, the cells can survive almost normally, as observed with moss *msh2* mutant cells exposed to cisplatin. We suggest that in wild-type cells, the DNA lesions caused by cisplatin trigger cell death and/or prolonged cell-cycle arrest through PpMSH2. We have evidence that the cell cycle is perturbed in the absence of PpMSH2: during the regeneration of protoplasts, *Ppmsh2* mutants showed a slightly higher rate of cell division compared with the wild type. This

suggests that *Ppmsh2* mutants may have an accelerated cell cycle, which may be explained if there was shorter arrest at cell-cycle checkpoints. Indeed, in mice it has been shown that after DNA damage, the absence of MSH2 results in premature release from the early G2/M arrest and an inability to activate properly the checkpoint kinase proteins (40). It was suggested that an active MSH2 is required for a correct response to DNA damage in the G2 phase of the cell cycle, possibly connecting DSB repair to checkpoint signaling. Moreover, in human, MMR is required for S-phase and G2-M checkpoint regulation (56,57). Consistent with these findings, we suggest that PpMSH2 is required for efficient cell-cycle arrest induced by DNA damage and may be a key component acting on DNA damage-activated checkpoints.

PpMSH2 is involved in HR and is essential to homeologous recombination

We examined the influence of MMR on HR in *P.patens* by assaying the frequency of recombination between a foreign DNA fragment released *in vivo* and a genomic target sequence. We found that the frequency of GT via HR between identical DNA was decreased 1.8-fold in the *Ppmsh2*-defective cells compared with the wild type. In mice, *msh2* mutants show a slight decrease of GT efficiency with homologous fragment compared with wild-type mice, and this decrease is comparable with our results (1.5-fold) (7). In yeast, a recent study has shown that the frequency of GT was reduced 3- to 4-fold in the *msh2* strain (58). Together with our results, these suggest that MSH2 in *P.patens* is probably involved in mechanisms that regulate GT of perfectly matching sequences in the genome. Further analyses are needed to determine the mechanisms involved.

We tested the influence of MMR on homeologous recombination in *P.patens* by assaying the frequency of recombination between a mutated DNA fragment and a genomic target sequence. Our results show that DNA sequence identity is important to determine the efficiency of gene replacement in the wild type. We have also shown that lack of PpMSH2 allows homeologous sequences with up to 3% divergence to be as efficiently targeted as perfectly identical sequences to a genomic locus. This shows that PpMSH2 plays a major role to prevent recombination between homeologous sequences. This is consistent with the similar role described for MMR in *E.coli* (29), in *Trypanosoma* (30), in yeast (5) and in mouse cells (7,59,60), suggesting that this role of MSH2 is strongly preserved during evolution. However, this is the first time that MSH2 involvement in HR and homeologous recombination is shown in plants.

In conclusion, we have found that in moss, MSH2 is involved in mismatch recognition and repair that most likely results from DNA replication errors, and in the response to certain genotoxic agents. Moreover, MSH2 plays a role in HR and in the recognition of mismatches that occur during heteroduplex formation between two not perfectly complementary DNA strands. These mechanisms are essential for maintaining genome integrity in all organisms and to establish interspecific barrier. This is particularly true for plants as they are unable to move and must cope with exposure to environmental mutagens. Thus, an efficient mechanism for genomic stability is needed in plants, and even more in mosses, where the major developmental stage of the life cycle is the haploid gametophyte. This is emphasized by the dramatic deleterious effect on development observed in an *msh2 P.patens* mutant compared with its *A.thaliana* counterpart. Our results show for the first time, the crucial role of MMR in a pluricellular organism where HR seems to be one of the major pathways to repair DNA lesions.

ACKNOWLEDGEMENTS

The authors thank Mr Favodon, (Institut Curie, Orsay, France), for help with the ^{137}Cs irradiator for gamma radiations assays. The authors thank Dr Michel Laloue (INRA Versailles, France) for providing the 2-Fluoroadenine. The authors thank Marie-Pascale Doutriaux, Mathilde Grelon, Christine Mézard and Raphaël Mercier for suggestions and discussions on the manuscript. This work was supported by grant from the Institut National de la Recherche Agronomique and Cellectis SA (Romainville, France). Funding to pay the Open Access publication charges for this article was provided by Institut National de la Recherche Agronomique.

Conflict of interest statement. None declared.

REFERENCES

1. Modrich,P. and Lahue,R. (1996) Mismatch repair in replication fidelity, genetic recombination, and cancer biology. *Annu. Rev. Biochem.*, **65**, 101–133.
2. Harfe,B.D. and Jinks-Robertson,S. (2000) DNA mismatch repair and genetic instability. *Annu. Rev. Genet.*, **34**, 359–399.
3. Kolodner,R. (1996) Biochemistry and genetics of eukaryotic mismatch repair. *Genes Dev.*, **10**, 1433–1442.
4. Schofield,M.J. and Hsieh,P. (2003) DNA mismatch repair: molecular mechanisms and biological function. *Annu. Rev. Microbiol.*, **57**, 579–608.
5. Negritto,M.T., Wu,X., Kuo,T., Chu,S. and Bailis,A.M. (1997) Influence of DNA sequence identity on efficiency of targeted gene replacement. *Mol. Cell. Biol.*, **17**, 278–286.
6. Sia,E.A., Kokoska,R.J., Dominska,M., Greenwell,P. and Petes,T.D. (1997) Microsatellite instability in yeast: dependence on repeat unit size and DNA mismatch repair genes. *Mol. Cell. Biol.*, **17**, 2851–2858.
7. de Wind,N., Dekker,M., Berns,A., Radman,M. and te Riele,H. (1995) Inactivation of the mouse Msh2 gene results in mismatch repair deficiency, methylation tolerance, hyperrecombination, and predisposition to cancer. *Cell*, **82**, 321–330.
8. Greene,C.N. and Jinks-Robertson,S. (2001) Spontaneous frameshift mutations in *Saccharomyces cerevisiae*: accumulation during DNA replication and removal by proofreading and mismatch repair activities. *Genetics*, **159**, 65–75.
9. Degtyareva,N.P., Greenwell,P., Hofmann,E.R., Hengartner,M.O., Zhang,L., Culotti,J.G. and Petes,T.D. (2002) *Caenorhabditis elegans* DNA mismatch repair gene msh-2 is required for microsatellite stability and maintenance of genome integrity. *Proc. Natl Acad. Sci. USA*, **99**, 2158–2163.
10. Hoffman,P.D., Leonard,J.M., Lindberg,G.E., Bollmann,S.R. and Hays,J.B. (2004) Rapid accumulation of mutations during seed-to-seed propagation of mismatch-repair-defective Arabidopsis. *Genes Dev.*, **18**, 2676–2685.
11. Schaefer,D. (2002) A new moss genetics: targeted mutagenesis in *Physcomitrella patens*. *Annu. Rev. Plant Biol.*, **53**, 477–501.
12. Brun,F., Gonneau,M., Doutriaux,M.P., Laloue,M. and Nogué,F. (2001) Cloning of the PpMSH-2 cDNA of Physcomitrella patens, a moss in which gene targeting by homologous recombination occurs at high frequency. *Biochimie*, **83**, 1003–1008.
13. Ashton,N.W. and Cove,D.J. (1977) The isolation and preliminary characterisation of auxotrophic and analogue resistant mutants of the moss, *Physcomitrella patens*. *Mol. Gen. Genet.*, 87–95.
14. Asthon,N.W., Grimsley,N. and Cove,D.J. (1979) Analysis of gametopytic development in the moss, *Physcomitrella patens*, using auxin and cytokinn resistants mutants. *Planta*, 427–435.

15. Sambrook,J., Frisch,E.F. and Maniatis,T. (1989) *Molecular Cloning: A Laboratory manual*. Cold Spring Harbor Laboratory Press, NY.
16. Cadwell,R.C. and Joyce,G.F. (1994) Mutagenic PCR. *PCR Methods Appl*., **3**, S136–S140.
17. Bilang,R., Iida,S., Peterhans,A., Potrykus,I. and Paszkowski,J. (1991) The 3′ terminal region of the hygromycin-B-resistance gene is important for its activity in *Escherichia coli* and *Nicotiana tabacum*. *Gene*, **100**, 247–250.
18. Schaefer,D.G. and Zrÿd,J.P. (1997) Efficient gene targeting in the moss *Physcomitrella patens*. *Plant J*., **11**, 1195–1206.
19. Sauer,B. (1993) Manipulation of transgenes by site-specific recombination: use of Cre recombinase. *Methods Enzymol*., **225**, 890–900.
20. Albert,H., Dale,E.C., Lee,E. and Ow,D.W. (1995) Site-specific integration of DNA into wild-type and mutant lox sites placed in the plant genome. *Plant J*., **7**, 649–659.
21. Schaefer,D.G. and Zryd,J.P. (2001) The moss *Physcomitrella patens*, now and then. *Plant Physiol*., **127**, 1430–1438.
22. Fedier,A. and Fink,D. (2004) Mutations in DNA mismatch repair genes: implications for DNA damage signaling and drug sensitivity (review). *Int. J. Oncol*., **24**, 1039–1047.
23. Hutchinson,F. (1985) Chemical changes induced in DNA by ionizing radiation. *Prog. Nucleic Acid Res. Mol. Biol*., **32**, 115–154.
24. Ward,J.F. (1988) DNA damage produced by ionizing radiation in mammalian cells: identities, mechanisms of formation, and reparability. *Prog. Nucleic Acid Res. Mol. Biol*., **35**, 95–125.
25. Jasen,M.A.K., Gaba,V. and Greengerg,B.M. (1998) Higher plants and UV-B radiation: balancing damage, repair and acclimation. *Trends Plant Sci*., **3**, 131–135.
26. Aebi,S., Kurdi-Haidar,B., Gordon,R., Cenni,B., Zheng,H., Fink,D., Christen,R.D., Boland,C.R., Koi,M., Fishel,R. *et al*. (1996) Loss of DNA mismatch repair in acquired resistance to cisplatin. *Cancer Res*., **56**, 3087–3090.
27. Humbert,O., Fiumicino,S., Aquilina,G., Branch,P., Oda,S., Zijno,A., Karran,P. and Bignami,M. (1999) Mismatch repair and differential sensitivity of mouse and human cells to methylating agents. *Carcinogenesis*, **20**, 205–214.
28. Jovtchev,G., Menke,M. and Schubert,I. (2001) The comet assay detects adaptation to MNU-induced DNA damage in barley. *Mutation Res*., **493**, 95–100.
29. Rayssiguier,C., Thaler,D.S. and Radman,M. (1989) The barrier to recombination between *Escherichia coli* and *Salmonella typhimurium* is disrupted in mismatch-repair mutants. *Nature*, **342**, 396–401.
30. Bell,J.S. and McCulloch,R. (2003) Mismatch repair regulates homologous recombination, but has little influence on antigenic variation, in *Trypanosoma brucei*. *J. Biol. Chem*., **278**, 45182–45188.
31. Buermeyer,A.B., Deschenes,S.M., Baker,S.M. and Liskay,R.M. (1999) Mammalian DNA mismatch repair. *Annu. Rev. Genet*., **33**, 533–564.
32. Schaaper,R.M. and Dunn,R.L. (1987) Spectra of spontaneous mutations in *Escherichia coli* strains defective in mismatch correction: the nature of *in vivo* DNA replication errors. *Proc. Natl Acad. Sci. USA*, **84**, 6220–6224.
33. Rudolph,C., Kunz,C., Parisi,S., Lehmann,E., Hartsuiker,E., Fartmann,B., Kramer,W., Kohli,J. and Fleck,O. (1999) The msh2 gene of *Schizosaccharomyces pombe* is involved in mismatch repair, mating-type switching, and meiotic chromosome organization. *Mol. Cell. Biol*., **19**, 241–250.
34. Denver,D.R., Feinberg,S., Estes,S., Thomas,W.K. and Lynch,M. (2005) Mutation rates, spectra, and hotspots in mismatch repair-deficient *Caenorhabditis elegans*. *Genetics*.
35. Malkhosyan,S., McCarty,A., Sawai,H. and Perucho,M. (1996) Differences in the spectrum of spontaneous mutations in the hprt gene between tumor cells of the microsatellite mutator phenotype. *Mutat Res*., **316**, 249–259.
36. Reenan,R.A.G. and Kolodner,R.D. (1992) Characterization of insertion mutations in the *Saccharomyces cerevisiae* Msh1 and Msh2 genes—evidence for separate mitochondrial and nuclear functions. *Genetics*, **132**, 975–985.
37. Peters,A.C., Young,L.C., Maeda,T., Tron,V.A. and Andrew,S.E. (2003) Mammalian DNA mismatch repair protects cells from UVB-induced DNA damage by facilitating apoptosis and p53 activation. *DNA Repair (Amst.)*, **2**, 427–435.
38. Fritzell,J.A., Narayanan,L., Baker,S.M., Bronner,C.E., Andrew,S.E., Prolla,T.A., Bradley,A., Jirik,F.R., Liskay,R.M. and Glazer,P.M. (1997) Role of DNA mismatch repair in the cytotoxicity of ionizing radiation. *Cancer Res*., **57**, 5143–5147.
39. DeWeese,T.L., Shipman,J.M., Larrier,N.A., Buckley,N.M., Kidd,L.R., Groopman,J.D., Cutler,R.G., te Riele,H. and Nelson,W.G. (1998) Mouse embryonic stem cells carrying one or two defective Msh2 alleles respond abnormally to oxidative stress inflicted by low-level radiation. *Proc. Natl Acad. Sci. USA*, **95**, 11915–11920.
40. Franchitto,A., Pichierri,P., Piergentili,R., Crescenzi,M., Bignami,M. and Palitti,F. (2003) The mammalian mismatch repair protein MSH2 is required for correct MRE11 and RAD51 relocalization and for efficient cell cycle arrest induced by ionizing radiation in G2 phase. *Oncogene*, **22**, 2110–2120.
41. Aquilina,G., Crescenzi,M. and Bignami,M. (1999) Mismatch repair, G(2)/M cell cycle arrest and lethality after DNA damage. *Carcinogenesis*, **20**, 2317–2326.
42. Flores,C. and Engels,W. (1999) Microsatellite instability in Drosophila spellchecker1 (MutS homolog) mutants. *Proc. Natl Acad. Sci. USA*, **96**, 2964–2969.
43. Karran,P. and Marinus,M.G. (1982) Mismatch correction at O6-methylguanine residues in *E.coli* DNA. *Nature*, **296**, 868–869.
44. Bell,J.S., Harvey,T.I., Sims,A.M. and McCulloch,R. (2004) Characterization of components of the mismatch repair machinery in *Trypanosoma brucei*. *Mol. Microbiol*., **51**, 159–173.
45. Cejka,P., Mojas,N., Gillet,L., Schar,P. and Jiricny,J. (2005) Homologous recombination rescues mismatch-repair-dependent cytotoxicity of S(N)1-type methylating agents in *S.cerevisiae*. *Curr. Biol*., **15**, 1395–1400.
46. Calmann,M.A., Nowosielska,A. and Marinus,M.G. (2005) Separation of mutation avoidance and antirecombination functions in an *Escherichia coli* mutS mutant. *Nucleic Acids Res*., **33**, 1193–1200.
47. Fram,R.J., Cusick,P.S., Wilson,J.M. and Marinus,M.G. (1985) Mismatch repair of *cis*-diamminedichloroplatinum(II)-induced DNA damage. *Mol. Pharmacol*., **28**, 51–55.
48. Fink,D., Zheng,H., Nebel,S., Norris,P.S., Aebi,S., Lin,T.P., Nehme,A., Christen,R.D., Haas,M., MacLeod,C.L. *et al*. (1997) *In vitro* and *in vivo* resistance to cisplatin in cells that have lost DNA mismatch repair. *Cancer Res*., **57**, 1841–1845.
49. Claij,N. and te Riele,H. (2004) Msh2 deficiency does not contribute to cisplatin resistance in mouse embryonic stem cells. *Oncogene*, **23**, 260–266.
50. Augusto-Pinto,L., Teixeira,S.M., Pena,S.D. and Machado,C.R. (2003) Single-nucleotide polymorphisms of the *Trypanosoma cruzi* MSH2 gene support the existence of three phylogenetic lineages presenting differences in mismatch-repair efficiency. *Genetics*, **164**, 117–126.
51. Drotschmann,K., Topping,R.P., Clodfelter,J.E. and Salsbury,F.R. (2004) Mutations in the nucleotide-binding domain of MutS homologs uncouple cell death from cell survival. *DNA Repair (Amst.)*, **3**, 729–742.
52. Lehmann,A.R. (2005) Replication of damaged DNA by translesion synthesis in human cells. *FEBS Lett*., **579**, 873–876.
53. Hoffmann,J.S., Locker,D., Villani,G. and Leng,M. (1997) HMG1 protein inhibits the translesion synthesis of the major DNA cisplatin adduct by cell extracts. *J. Mol. Biol*., **270**, 539–543.
54. Lindahl,T. and Wood,R.D. (1999) Quality control by DNA repair. *Science*, **286**, 1897–1905.
55. Liu,Z., Hossain,G.S., Islas-Osuna,M.A., Mitchell,D.L. and Mount,D.W. (2000) Repair of UV damage in plants by nucleotide excision repair: Arabidopsis UVH1 DNA repair gene is a homolog of *Saccharomyces cerevisiae* Rad1. *Plant J*., **21**, 519–528.
56. Brown,K.D., Rathi,A., Kamath,R., Beardsley,D.I., Zhan,Q., Mannino,J.L. and Baskaran,R. (2003) The mismatch repair system is required for S-phase checkpoint activation. *Nature Genet*., **33**, 80–84.
57. Yan,T., Schupp,J.E., Hwang,H.S., Wagner,M.W., Berry,S.E., Strickfaden,S., Veigl,M.L., Sedwick,W.D., Boothman,D.A. and Kinsella,T.J. (2001) Loss of DNA mismatch repair imparts defective cdc2 signaling and G(2) arrest responses without altering survival after ionizing radiation. *Cancer Res*., **61**, 8290–8297.
58. Langston,L.D. and Symington,L.S. (2005) Opposing roles for DNA structure-specific proteins Rad1, Msh2, Msh3, and Sgs1 in yeast gene targeting. *EMBO J*., **24**, 2214–2223.
59. Elliott,B. and Jasin,M. (2001) Repair of double-strand breaks by homologous recombination in mismatch repair-defective mammalian cells. *Mol. Cell. Biol*., **21**, 2671–2682.
60. Abuin,A., Zhang,H. and Bradley,A. (2000) Genetic analysis of mouse embryonic stem cells bearing Msh3 and Msh2 single and compound mutations. *Mol. Cell. Biol*., **20**, 149–157.